THIS BOOK IS OF POOR LEGIBILITY DUE TO LIGHT PRINTING THROUGH OUT IT'S ENTIRETY.

THIS IS AS RECEIVED FROM THE CUSTOMER.

PETROGENESIS OF THE SPANISH PEAKS IGNEOUS COMPLEX, COLORADO: MAJOR ELEMENT, RARE EARTH ELEMENT, AND STRONTIUM ISOTOPIC DATA

by

Bill W. Arnold

B. S., Kansas State University, 1973

A MASTER'S THESIS

submitted in partial fulfillment of the

requirements for the degree

MASTER OF SCIENCE

Department of Geology

KANSAS STATE UNIVERSITY
Manhattan, Kansas

1977

Approved by:

Robert Cullers
Major Professor

TABLE OF CONTENTS

TABLES

Figures

INTRODUCTION

The Spanish Peaks igneous complex of Colorado is a compositionally diverse group of stocks, dikes, and other intrusions of Tertiary age, ranging from silicic to ultramafic in composition. Knopf (1936) recognized and classified the great diversity of igneous rock types in the complex. He attributed this diversity to magmatic differentiation at the two main centers of intrusion and to variations in rate of cooling and water content. He also related chemical peculiarities of the Spanish Peaks complex with other igneous rocks along the east flank of the Rocky Mountains.

Johnson (1968), who performed a more complete survey of mapping, igneous petrography, and chemical analysis of the complex, stated that the general order of intrusion was from silicic to mafic; however, the intrusion of the radial dikes as a separate group is from mafic to silicic.

Using Sr isotopic data and K, Rb, Sr, and Ba concentrations, Jahn (1973) constructed a model for the formation of the Spanish Peaks complex. His Sr isotopic data ruled out a comagmatic origin for all the igneous rocks of the complex, which precludes the fractional crystallization of a single parent magma as suggested by Knopf (1936). Also, the Sr isotopic initial ratios from the Spanish Peaks complex are similar to other Cenozoic igneous rocks of the southern Rocky Mountain region, suggesting similar modes of origin (Jahn, 1973; Doe, 1968).

Jahn (1973) suggested that there were at least two separate sources for the igneous rocks at the Spanish Peaks complex. He hypothesized that the lamprophyric magmas could have been derived from phlogopite-bearing hornblende peridotite by a small degree of partial melting in the upper

mantle and that the granitic magma could have formed by partial melting of amphibolite or basalt in the lower crust. Mixing of these two independant magmas could then form the intermediate rock types.

This study determines the distribution of the rare earth elements (REE) in representative samples of the Spanish Peaks igneous complex and uses these data in conjunction with major element analyses and Sr isotopic data to test various models for the origin of the complex. By assuming a given mineralogy for the source rock and a given degree of partial melting or fractional crystallization the hypothetical REE composition of the melt can be calculated using known distribution coefficients. these hypthetical compositions are then compared with the compositions of the igneous rocks to test the given model. Sr^{87}/Sr^{86} initial ratios are used to limit possible sources.

GEOLOGY

The Spanish Peaks igneous complex of south-central Colorado is a classic area of shallow Tertiary intrusions. Stormer (1972) gave K-Ar ages of 22 - 25 million years for samples from this complex. The complex consists of two main intrusive stocks which form East and West Spanish Peaks, a system of radiating and subparallel dikes, and some smaller stocks and plugs (Figure 1).

The igneous rock types are petrographically and chemically diverse, and they make up a continous gradation from silicic to ultramafic, with the most abundant type being syenodiorite (Johnson, 1968; Knopf, 1936). The general order of intrusion was granitic to mafic as determined by cross-cutting relationships (Johnson, 1961).

Figure 1

Geologic map of the Spanish Peaks igneous complex with sample localities indicated.

SPANISH PEAKS REGION, COLORADO

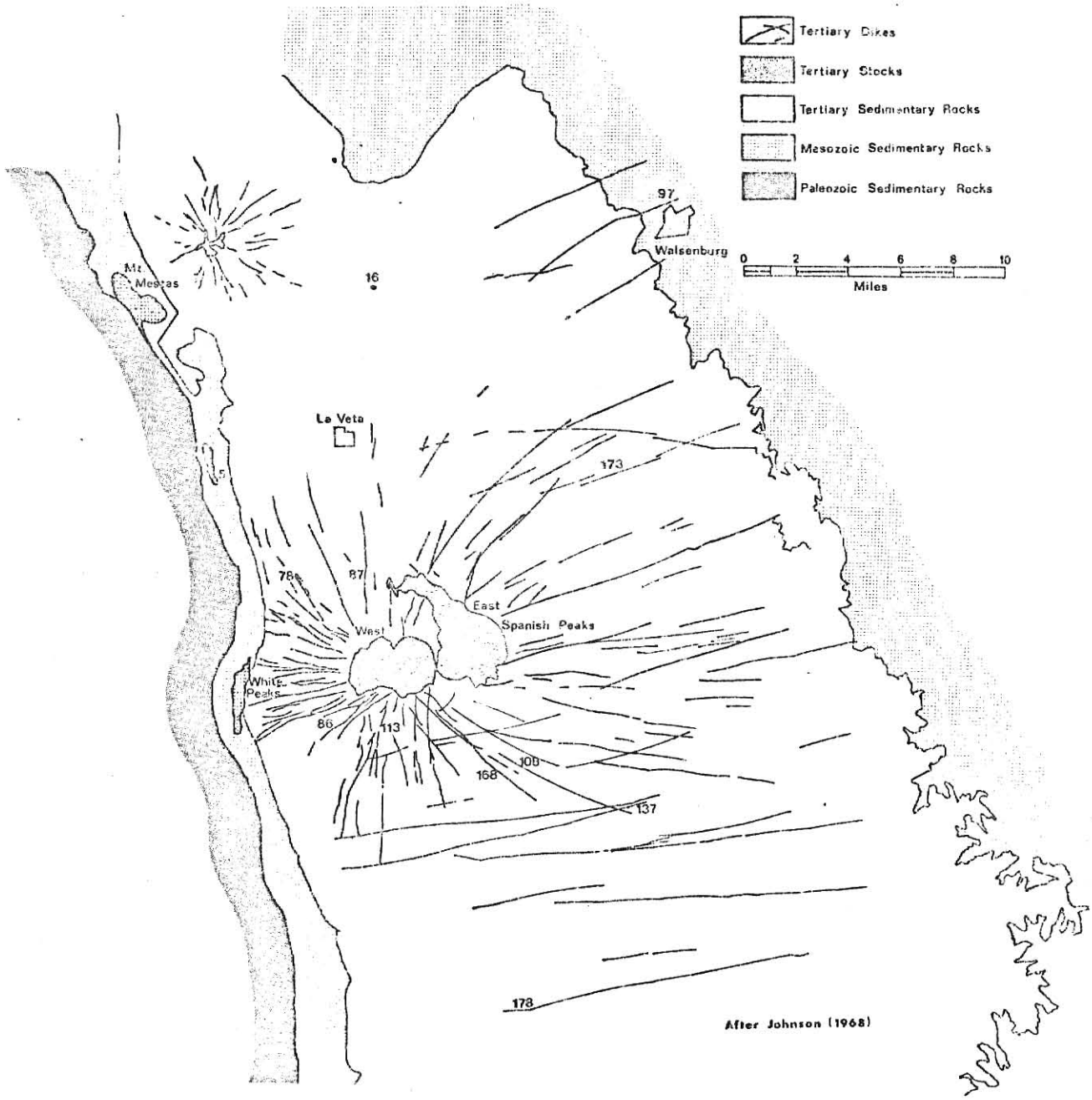

The Spanish Peaks are approximately on the axis of the La Veta Syncline which is the structural feature that forms the northern extension of the Ratone Basin. The La Veta Syncline is a broad, asymmetric syncline with a steeply dipping western limb and gently dipping eastern limb. Igneous rocks of the complex intruded sedimentary rocks ranging from Pennsylvanian to Eocene (Johnson, 1968). Johnson (1961) stated that the dike pattern was controlled by a combination of the joint patterns generated by regional folding and by the emplacement of the East and West Spanish Peaks stocks.

EXPERIMENTAL METHODS

Sample Preparation

Hand specimens of some samples analyzed in this study were collected by the author in the field and trimmed to remove weathered surfaces. Thin sections were prepared and described (Appendix I). A portion of the hand specimen was ground in a tungsten carbide-lined ball mixer mill and sieved through a 100 mesh sieve. Other samples were obtained as sample splits from Ross Johnson of the United States Geological Survey, Denver, Colorado (Johnson, 1968).

Several Samples contain significant amounts of alteration or secondary minerals (Appendix I). REE should be relatively unaffected by most weathering processes, unless weathering is severe (Philpotts, et al, 1970; Ronov, et al, 1967). The Sr^{87}/Sr^{86} initial ratios in such relatively young rocks would not be significantly affected by the preferential movement of Rb or Sr because of the relatively long half-life of Rb^{87}, unless the intrusion were contaminated by the introduction of Sr with a different isotopic composition than the host rock.

Atomic Absorption Spectrophotometry and Ignition

Atomic absorption spectrophotometry (AA) was used to determine the concentrations of the major elements in the samples collected by the author. The technique consists of dissolution of a powdered sample in a teflon-lined bomb with HF acid and aqua regia followed by the addition of boric acid and dilution with deionized water (Buckley, et al, 1971).

The results of AA analyses for three U.S.G.S. standard rocks are compared to average values for each element from Flanagan (1969) in Table 1. The agreement between the author's values and the standard analyses for most elements is good. The greatest absolute errors were in the SiO_2 values which are low by approximately 1.7 percent. Silicon analysis by AA is difficult and improvement was noticed with certain refinements. A detailed description of AA techniques is given in Appendix II.

Ignition was performed on samples to determine the total volatile content. Approximately 0.5 gram of sample was placed in a preweighed platinum crucible and was weighed to the nearest 0.0001 g. The crucible was placed in a muffle furnace at 1000°C for 30 minutes and then was cooled in a desiccator. The crucible was reweighed and the percentage ignition calculated.

Mass Spectrometry

Strontium isotopic data were obtained from three granitic samples by mass spectrometry using techniques similar to Methot (1973). The Rb and Sr concentrations were obtained by x-ray fluorescence. The error in the Rb/Sr ratio by this technique has been estimated as 2.5 percent.

Replicate analyses of Sr^{87}/Sr^{86} ratio for the Eimer and Amend $SrCO_3$ standard gave values of 0.7083 $\pm$ 0.0006. A more detailed description of experimental methods is in Appendix II.

TABLE 1

Atomic Absorption Analyses of U.S.G.S. Standard Rocks (weight percent oxides)

oxide	G-2	AGV-1	BCR-1	G-2*	AGV-1*	BCR-1*
SiO_2	67.6	57.3	52.8	69.19	58.99	54.48
Al_2O_3	15.38	17.27	13.53	15.34	17.01	13.65
Fe as Fe_2O_3	2.66	6.78	13.70	2.76	6.80	13.50
MgO	0.73	1.48	3.38	0.78	1.49	3.28
CaO	2.01	4.76	6.88	1.98	4.98	6.95
Na_2O	4.18	4.29	3.26	4.15	4.33	3.31
K_2O	4.52	3.03	1.73	4.51	2.89	1.68
TiO_2	0.43	1.13	2.67	0.53	1.08	2.23
ignition	0.52	1.65	1.18	-	-	-
	98.03	97.69	99.13	99.24	97.57	99.08

* from Flanagan (1969)

Neutron Activation Analysis

The concentrations of the REE were determined by radiochemical neutron activation analysis (NAA) (Denechaud, et al, 1970). Powdered samples were sealed in polyethylene vials and irradiated in the reactor core. They were then removed and the REE were chemically separated as a group from the sample and precipitated as REE oxalates. The precipitate was mounted on cards and gamma-ray spectra were obtained on a Ge(Li) detector coupled with a 4096 channel analyzer. Peak areas of different elements for the samples were compared with standards to determine concentrations.

The results of Yeh (1973), using the same equipment and techniques as the author, are compared with the results of Haskin, et al, (1970) and Gordon, et al, (1968) for U.S.G.S. standard rock BCR-1 (Table 2). The agreement between the results of Yeh (1973) and Haskin, et al, (1970) is good. The lower agreement between Yeh (1973) and Gordon, et al, (1968) may be due to the lesser accuracy of instrumental NAA compared to radiochemical NAA. Appendix II contains a more detailed description of NAA techniques.

RESULTS

Introduction

Samples were selected for trace element analysis which are representative of major element compositions for the dikes and East and West Spanish Peaks. Microgranite samples were analyzed for the REE, major elements, and Sr isotopic composition because of their anomalously low REE contents.

TABLE 2

Abundances of the REE (ppm) in BCR-1

Reference	La	Ce	Sm	Eu	Gd	Tb	Ho	Yb	Lu
Yeh (1973) RNAA	26.40	54.9	7.25	2.05	8.91	1.21	1.54	3.33	0.540
Haskin, et al (1970) RNAA	25.18	54.22	7.23	1.966	8.02	1.154	1.342	3.48	0.526
Gordon, et al (1968) INAA	23	46	5.9	1.95	-	1.0	-	3.2	0.60

Major Elements

Samples representing a range of SiO_2 contents were chosen for analysis. Silicic rocks were oversampled because a low REE content was found for one silicic sample and the author wished to delineate between high REE silicics and low REE silicics.

Major elements determined in this study are summarized in Table 3A and other major element analyses of samples for which REE data were obtained are in Table 3B (Johnson, 1968). Samples #97, #168, and #173 are classified as lamprophyres; #178 as a gabbro; #86, #108, #113, and #137 as intermediates; and E. Spanish Peak, Mount Mestas, #78, #87, S. White Peak, #5, and #16 as silicic rocks.

Major element data are plotted on a modified AFM diagram (Figure 2), indicating a trend from alkali-rich rocks to Fe and Mg Rich rocks with decreasing SiO_2 content. This trend is very similar to calc-alkaline igneous rocks of oceanic island arcs (Green and Ringwood, 1968). Most samples plotted fall on a general trend between the granitic field and the lamprophyric field; however, several intermediate and mafic composition samples are scattered outside this trend.

A similar trend on the AFM diagram was noted by Siems (1968) for volcanic rocks of rhyolitic to intermediate composition of the Silver Cliff-Rosita Hills district which is a nearby area of Cenozoic volcanic flows. These rocks are of similar age to the Spanish Peaks, but any major mafic or ultramafic rock types are lacking.

The C.I.P.W. normative compositions calculated from major element data are in Table 4. All silicic and intermediate samples contain quartz in the norm. The three lamprophyres have normative nepheline and olivine.

TABLE 3A

Atomic Absorption Analyses of Spanish Peaks Samples (weight percent oxides)

	Lamprophyres			silicic rocks		
oxides	#97	#168	#173	S. White Peak	#5	#16
SiO_2	40.3	45.2	43.6	67.9	74.9	73.8
Al_2O_3	10.92	11.34	12.13	14.32	13.34	14.21
Fe as Fe_2O_3	11.31	10.68	11.84	2.49	0.66	0.34
MgO	6.50	8.08	9.45	0.96	0.10	0.05
CaO	9.72	9.79	9.98	2.24	0.17	0.45
Na_2O	1.18	1.83	2.64	5.39	4.53	5.36
K_2O	5.73	4.02	2.46	2.84	4.46	4.31
TiO_2	3.64	3.07	2.64	0.17	<0.03	<0.03
ignition	6.38	5.23	3.41	1.02	0.69	0.39
total	96.31	99.24	98.15	97.33	98.85	98.91
$\frac{Na_2O + K_2O}{MgO + Fe_2O_3}$	0.388	0.312	0.240	2.39	11.83	24.79

TABLE 3B

Analyses of Spanish Peaks Samples Supplied by Ross B. Johnson (weight percent oxides)

	Silicic rocks				Intermediate rocks				Gabbro
oxides	E. Spanish Peak	Mount Mestas	#78	#87	#86	#108	#113	#137	#178
SiO_2	71.2	73.6	67.9	65.2	60.3	56	59.4	47.4	44
Al_2O_3	14.6	15.2	15.4	16.1	17	17.5	16.9	16.3	13.7
Fe_2O_3	1.1	.60	1.7	2.2	3.3	3.8	3	8.3	8
FeO	.98	.20	1.4	1.8	1.8	2.7	2.8	2	4
MgO	.71	.20	1.2	1.7	2	2.3	2.4	4.3	8.8
CaO	1.1	.83	2.1	2.8	3.3	4.3	4.2	7.8	9.5
Na_2O	3.6	4.3	4.3	5.1	4.7	5.2	4.5	3.7	2.2
K_2O	4.6	4.4	3.5	3.4	3.8	3.2	3.3	1.5	1.2
H_2O^-	.28	.23	.39	.21	.51	.69	.22	3.1	3
H_2O^+	.98	.74	1.1	.79	1.5	2.5	1.6	1.8	2.4
TiO_2	.33	.06	.49	.61	.86	1.3	1	2.1	1.7
P_2O_5	.12	.02	.21	.33	.41	.67	.55	1.5	.52
MnO	.10	.01	.01	.08	.12	.12	.11	.19	.18
CO_2	.22	.05	.05	.05	.56	.08	.05	.05	.86
total	100	100	100	100	100	100	100	100	100
$\frac{Na_2O + K_2O}{MgO + Fe_2O_3}$	2.83	8.51	1.75	1.44	1.16	0.923	0.916	0.351	0.160

from Johnson (1968)

TABLE 4

Normative Compositions of Spanish Peaks Samples (percent)

	#5	#16	Mt. * Mestas	East Spanish Peak *	South White Peak	#78*	#87*	#86*	#108*	#113*	#137*	#168	#178*	#173	#97
Q	31.01	25.21	30.16	31.16	20.51	24.68	15.16	14.14	3.32	9.61	2.45	0	0	0	0
C	0	0	2.02	2.50	0	1.53	0	1.44	0	0	0	0	0	0	0
or	26.35	25.63	26	27.18	16.79	20.68	20.09	22.45	18.91	19.50	8.86	23.80	7.09	14.57	10.62
ab	38.30	45.17	35.77	27.82	45.54	34.82	42.54	33.08	43.98	37.46	31.29	6.97	18.61	8.75	0
an	0.83	1.89	3.99	4.67	6.48	9.04	11.32	13.69	14.97	16.49	23.44	10.81	23.97	13.93	7.53
ne	0	0	0	0	0	0	0	0	0	0	0	4.60	0	7.36	5.40
nc	0	0	0.12	0.53	0	0.31	0.12	1.35	0	0.12	0	0	0	0	0
lc	0	0	0	0	0	0	0	0	0	0	0	0	0	0	18.27
mt	0.60	0.23	0.50	1.59	1.76	2.46	3.19	3.70	5.33	4.35	0.98	7.10	8.55	7.80	0
hm	0.03	0.06	0.25	0	0.50	0	0	0.75	0.13	0	7.62	0	2.10	0	7.86
il	0	0	0.11	0.63	0.32	0.93	1.16	1.63	2.47	1.90	3.99	5.84	3.23	5.02	6.55
pf	0	0	0	0	0	0	0	0	0	0	0	0	0	0	0.33
ap	0	0	0.05	0.28	0	0.50	0.78	0.97	1.59	1.30	3.55	0	1.23	0	0
cc	0	0	0	0	0	0	0	0	0.18	0	0	0	1.96	0	0
di	0	0.26	0	0	3.61	0	0.31	0	1.15	0.59	4.24	29.49	11.15	27.90	31.13
hy	0.25	0	0.50	2.30	0.73	3.44	4.71	4.98	5.19	6.91	8.74	0	16.74	0	0
ol	0	0	0	0	0	0	0	0	0	0	0	9.84	0	13.57	1.58
total	98.11	98.36	99.47	98.67	96.24	98.39	99.39	98.17	97.21	99.24	95.17	98.45	94.69	98.90	99.27

* taken from Johnson (1968)

Proportions of Fe_2O_3 and FeO for samples analyzed by the author were assumed to be the same rock types analyzed by Johnson (1968).

Figure 2

Modified AFM diagram using major element data from this study and from Johnson (1968).

⊙ data by the author

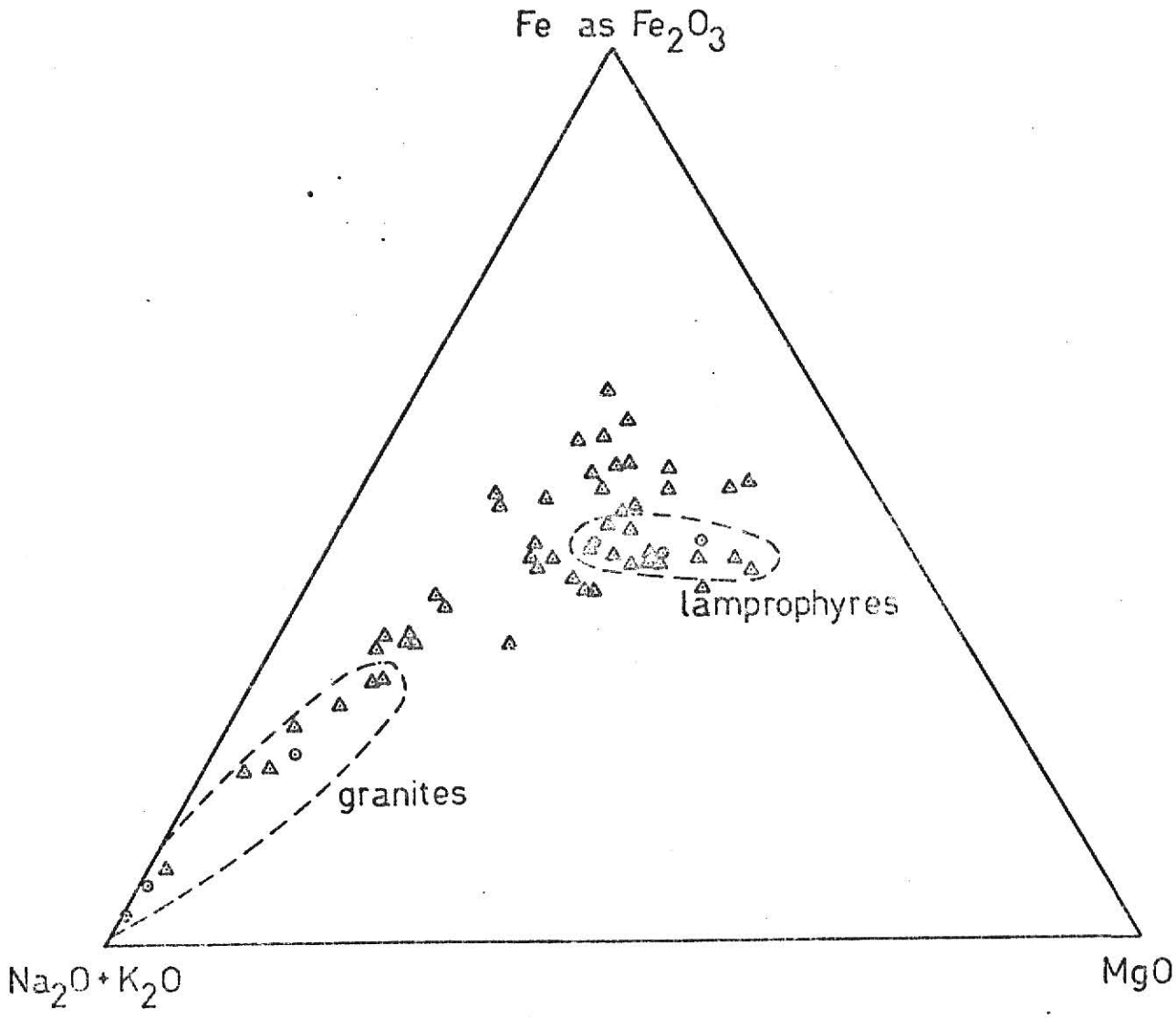

△ data from Johnson (1968)

Sr^{87}/Sr^{86} Initial Ratios

The Sr isotopic compositions of three granitic samples are in Table 5. These three samples are microgranites which occur as smaller satellite intrusions. Sr^{87}/Sr^{86} initial ratios for these samples were determined because their REE contents were anomalously low. To calculate the Sr^{87}/Sr^{86} initial ratios from the Sr^{87}/Sr^{86} present ratios an age of 25 million years was assumed, which is compatible with the K-Ar ages obtained by Stormer (1972). Sr^{87}/Sr^{86} initial ratios for these three samples (0.7070-0.7079) are identical, within limits of experimental error, with initial ratios obtained by Jahn (1973) for three other granitic rocks in the Spanish Peaks complex (0.7049-0.7085). Jahn (1973) reported a range of Sr^{87}/Sr^{86} initial ratios in twenty samples from a minimum of 0.7042 for a diorite to a maximum of 0.7090 for a syenodiorite, and he found that no isochron could be drawn using the whole rock data.

Rare Earth Elements

The REE data obtained by NAA are in Tables 6 and 7, and in Figures 3 and 4 as REE concentrations/chondrites versus REE atomic number. REE concentrations are normalized relative to chondritic meteorites (Haskin, et al, 1968), which are assumed to have a REE composition equal to the average terrestrial REE composition.

Some groups of samples classified on the basis of petrography and major element chemistry can be further subdivided on REE compositions. The mafic rocks include three lamprophyres and a gabbro. The lamprophyres are characterized by relatively high, variable absolute REE contents, high light REE/heavy REE ratios, and no Eu anomalies (Table 7). A Eu anomaly can be defined as a Eu concentration which is discontinuous with the other REE values on a chondrite-normalized curve. For this study a Eu

TABLE 5

Strontium Isotopic Ratios for Satellite Granites

sample	(Rb^{87}/Sr^{86})	(Sr^{87}/Sr^{86})	(Sr^{87}/Sr^{86}) initial
Mount Mestas	1.27	0.7082	0.7078 $\pm$ .0005
N. White Peak	0.20	0.7080	0.7079 $\pm$ .0005
Plug #16	2.24	0.7078	0.7070 $\pm$ .0005

TABLE 6

Rare Earth Element Concentrations (ppm) of Representative Samples, Spanish Peaks

Sample Number	La	Ce	Sm	Eu	Gd	Tb	Ho	Yb	Lu	ΣREE *	La/Lu	Eu/Sm	Eu/Eu*
#168	85.0	185	13.5	3.54	12	1.50	2.3	2.16	0.31	405.50	274	.262	1.00
#173	84.6	159	11.3	3.21	11	1.36	2.3	2.36	0.33	361.83	256	.284	1.00
#97	200.8	403	23.5	6.50	19	1.94	3.6	2.66	0.38	850.91	528	.277	1.09
#178	29.7	74.4	7.13	2.28	8.4	1.05	0.92	2.20	0.36	174.18	82.5	.320	1.05
#S6	80.3	130	6.77	1.88	8.3	0.957	1.3	3.21	0.58	296.62	138	.278	0.927
#113	71.4	113	6.01	1.64	7.4	0.804	1.1	2.22	0.44	259.24	162	.273	0.923
#108	61.6	108	6.27	1.93	6.1	0.910	1.0	1.96	0.36	242.06	171	.308	1.04
#137	55.7	108	8.48	2.97	9.4	1.26	1.4	2.54	0.45	254.56	124	.350	1.16
E. Sp. Peak	64.6	76.6	5.04	0.707	6.3	0.821	--	4.72	1.02	207.16	63.3	.140	0.449
#78	58.0	68.0	3.24	0.754	4.0	0.435	--	1.35	0.35	168.10	166	.233	0.786
#87	83.6	87.7	4.82	1.18	6.0	0.563	--	1.63	0.35	228.88	239	.245	0.871
S. White P.	18.8	40.5	3.08	0.911	2.4	0.361	0.35	0.94	0.15	90.21	125	.296	1.08
Mt. Mestas	4.06	6.23	0.96	0.349	--	0.212	--	0.91	0.21	21.42	19.3	.364	1.05
#5	1.39	4.45	0.78	0.299	1.5	0.204	0.23	0.43	0.08	14.34	17.4	.383	1.04
#16	0.59	3.33	0.90	0.348	2.1	0.358	0.48	1.03	0.18	15.56	3.3	.387	0.922

*Other REE not analyzed were estimated from chondrite-normalized curves

Figure 3a

(Top) Comparison of REE content in lamprophyric samples to chondrites.

- △ Dike #97 (minette)
- ○ Dike #168 (odinite)
- □ Dike #173 (monchiquite)

Figure 3b

(Bottom) Comparison of REE content in intermediate composition samples to chondrites.

- ○ Dike #86 (syenite prophyry)
- □ Dike #113 (syenodiorite porphyry)
- △ Dike #108 (syenodiorite porphyry)
- ▽ Dike #137 (syenodiorite)

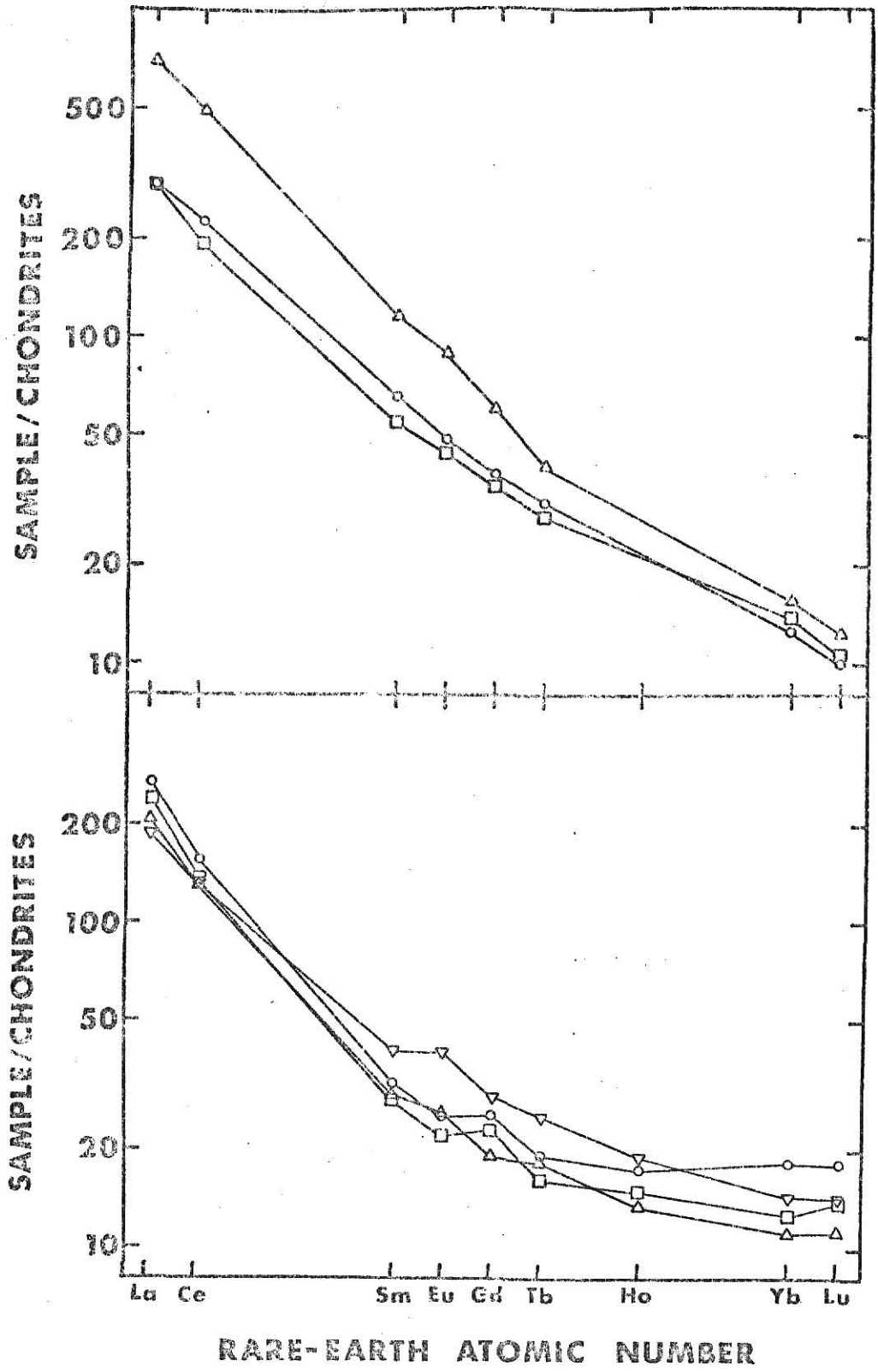
SAMPLE/CHONDRITES
500
200
100
50
20
10
SAMPLE/CHONDRITES
200
100
50
20
10
La
Ce
Sm
Eu
Gd
Tb
Ho
Yb
Lu
RARE-EARTH ATOMIC NUMBER

Figure 4a

(Top) Comparison of REE content in silicic samples to chondrites.

- o Dike #87 (granodiorite porphyry)
- ◘ East Spanish Peak (granite porphyry)
- ▵ Dike #78 (granite porphyry)
- ▽ Mount Mestas (microgranite)

Figure 4b

(Bottom) Comparison of REE content in satellite silicics and gabbro to chondrites.

- ▼ Dike #178 (gabbro porphyry)
- o South White Peak (granite)
- ◘ Stock #5 (granite)
- ▲ Plug #16 (microgranite)

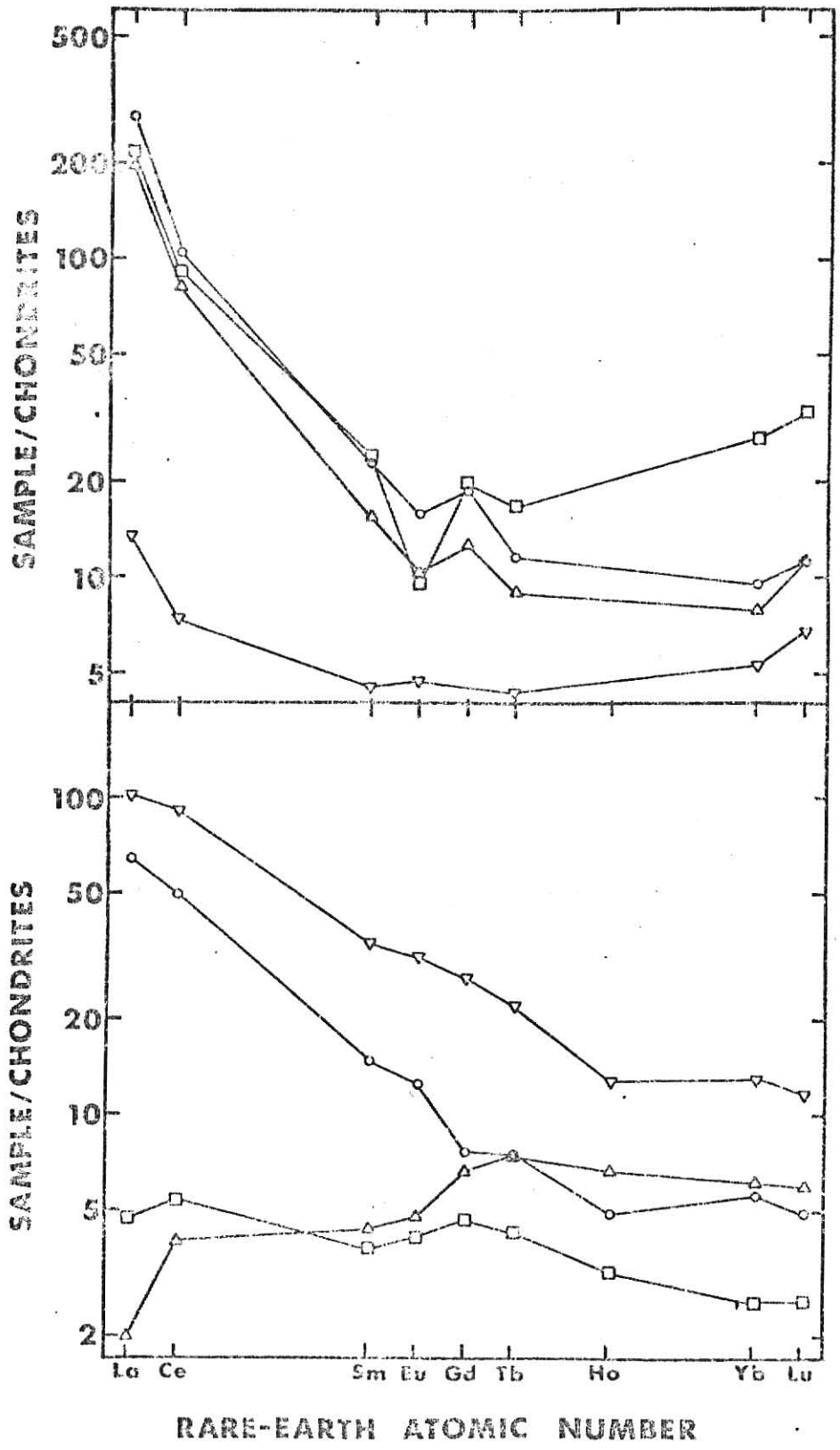
500
200
100
50
20
10
5
SAMPLE/CHONDRITES
100
50
20
10
5
2
SAMPLE/CHONDRITES
La Ce Sm Eu Gd Tb Ho Yb Lu
RARE-EARTH ATOMIC NUMBER

TABLE 7

Classification of Spanish Peaks Samples, Using REE Data

rock type	range of SiO_2 (percent)	range of $\frac{Na_2O+K_2O}{MgO+Fe_2O_3}$	range of Σ REE (ppm)	average $\pm\sigma$ Σ REE (ppm)	range of La/Lu	average $\pm\sigma$ La/Lu	range of Eu/Eu*
lamprophyres (#97, 168, 173)	40.3-45.2	0.240-0.388	361.8-850.9	539.4±270.6	256-528	353±152	1.00-1.09
gabbro (#178)	44	0.160	174.2	-	82.5	-	1.05
intermediates (#86, 108, 113, 137)	47.4-60.3	0.351-1.16	242.1-296.6	263.1±23.5	124-171	149±22	0.923-1.16
silicics (E.Span.Peak, #78, 87)	65.2-71.2	1.44-2.83	168.1-228.9	201.4±30.8	63.3-239	156±88	0.449-0.871
silicics (S. White P.)	67.9	2.39	90.2	-	125	-	1.08
silicics (Mt. Mestas, #5, 16)	73.6-74.9	8.51-24.79	14.3-21.4	17.1±3.8	3.3-19.3	13.3±8.7	0.922-1.05

concentration is considered to be a negative Eu anomaly if the Eu/Eu* ratio is greater than 1.2. Eu* is the Eu concentration obtained by interpolation from the other REE concentrations (mainly Sm, Gd, and Tb). The other mafic rock is a gabbro porphyry which has a lower light REE content, but otherwise similar REE composition as the lamprophyres.

Samples of intermediate composition have similar REE patterns to one another even though their SiO_2 contents range from 47.4-60.3 percent. The total REE content and light REE/heavy REE ratios (La/Lu ratios) of these samples are significantly lower than the lamprophyres (Table 7).

The silicic dikes #87 and #78 and East Spanish Peak granite have lower, but similar, overall REE concentrations to the lamprophyres and intermediate rocks. Dikes #87 and #78 have no Eu anomalies, but East Spanish Peak has a negative Eu anomaly.

The other silicic intrusions, Mount Mestas, the smaller satellite bodies #5 and #16 and to a lesser extent South White Peak, are characterized by much lower total REE content, no Eu anomalies and lower light REE/heavy REE ratios than the other silicic rocks (Table 7).

DISCUSSION

Introduction

A reasonable model for the orgin of the Spanish Peaks igneous complex must explain known field relationships, petrography, experimental petrology, geochemical and isotopic data. The basic model being tested is that the complex formed by partial melting of two sources and by mixing of the magmas. The lamprophyres formed by partial melting of phlogopite-bearing hornblende peridotite, the granites by partial melting of amphibolite or granulite, and the intermediate compositions by mixing of these two magmas (Jahn, 1973).

Formation of Lamprophyres and Gabbro

Several mechanisms have been proposed for the generation of lamprophyric magmas. Experimental partial melting a garnet peridotite at high pressure followed by fractionation can yield a lamprophyric magma (O'Hara and Yoder, 1967). Using Sr isotopic and trace element data, Jahn (1973) concluded that the source of the lamprophyric magmas of the Spanish Peaks complex was the partial melting of the phlogopite-bearing hornblende peridotite in the upper mantle. The alkali-rich lamprophyres can be explained by this process; but not by simple fractionation of a single magma as proposed by Knopf (Jahn, 1973). The Sr isotopic and trace element data of Jahn (1973) do not support the hypothesis of fractionation of a single magma to produce the range in composition at Spanish Peaks.

The REE data are compatible with the proposed partial melting of peridotite for the formation of the lamprophyric magmas. The partial melting relationships of Haskin, et al (1970) are used to test this model. Equation (1) summarizes these relationships.

$$C_P/C_A = (1-(1-X)^D)/X \qquad (1)$$

Where;

C_P = concentration of the trace element in the melt

C_A = average concentration of the trace element in the system

X = the fraction melted

D = bulk distribution coefficient for the trace element

The distribution coefficient is defined as the ratio of the concentration in the solid phase of the trace element to the concentration in the melt. Minerals with distribution coefficients greater than one tend to concentrate the trace element relative to the melt and minerals with distribution coef-

ficients less than one tend to enrich the melt in the trace element relative to the mineral. The bulk distribution coefficients for the REE are calculated assuming non-modal fractional melting. The bulk distribution coefficients are recalculated for each different degree of partial melting to reflect the changing proportions of minerals as certain minerals are preferentially melted. The distribution coefficients of Higuchi and Nagasawa (1969), Philpotts and Schnetzler (1970), Schnetzler and Philpotts (1968), and Schnetzler and Philpotts (1970) are used (Appendix III).

The first of two models for the formation of the lamprophyres (model A) assumes the following composition for the hornblende peridotite: 0.5 percent phlogopite, 10 percent hornblende, 20 percent diopside, and 69.5 percent olivine. This is similar to the model peridotite mineralogy proposed by Jahn (1973). The hydrous phases (phlogopite and hornblende) are assumed to melt first followed by proportional melting of diopside and olivine, so that after 3 percent partial melting the proportions of minerals in the solid phase would be 7.7 percent hornblende, 20.6 percent diopside, and 71.6 percent olivine. The upper portion of the field of REE distributions for high temperature-high pressure peridotites is in Figure 5 (Loubet, et al, 1975; Philpotts, et al, 1972; Reid and Frey, 1971). Because the model of Jahn (1973) locates the hornblende peridotite source in the upper mantle it can be reasonably assumed that the peridotite could be enriched in the REE. There are indications that the upper mantle is heterogeneous and chemically differentiated (Ringwood, 1975). In this case the parent peridotite is assumed to be at the upper limit of the field of REE content of peridotites. The REE composition of the magma predicted by 3 percent partial melting of Model A peridotite does not agree well with actual lamprophyre REE distributions for the heavy

Figure 5

Theoretical REE compositions of melts formed by 3 percent partial melting of model A peridotite and 3 percent, 5 percent, 10 percent, and 20 percent partial melting of model B peridotite. The range of REE compositions from this study for the lamprophyres is shaded. The REE distribution for gabbro sample #178 is shown as a dashed line. After 3 percent melting the proportions of minerals in the residual phase of model B peridotite would be 7.2 percent diopside, 2.1 percent garnet, 23.7 percent orthopyroxene, and 68.4 percent olivine. After 10 percent partial melting the proportions would be 2.2 percent garnet, 25.6 percent orthopyroxene, and 72.2 percent olivine.

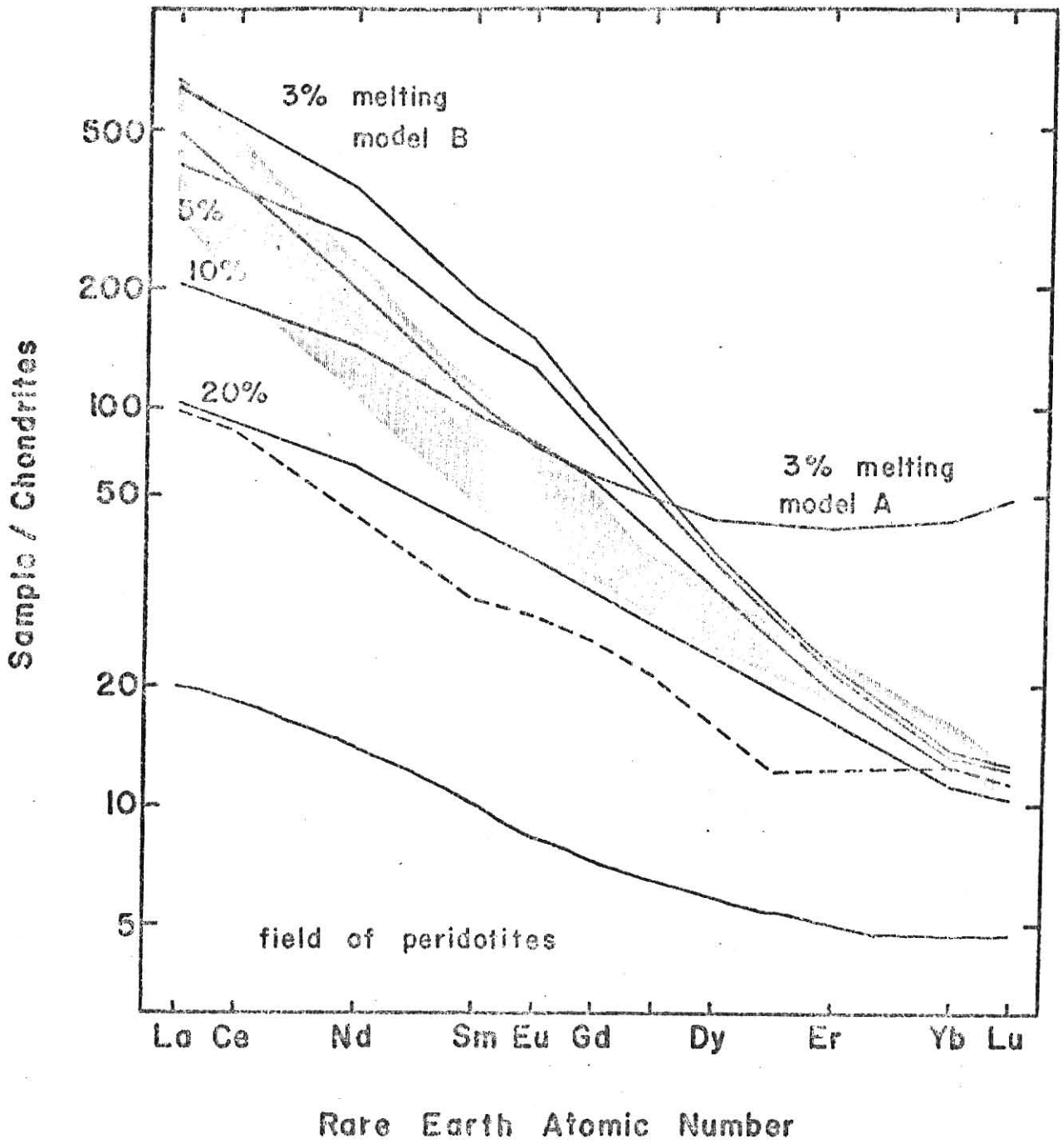
3% melting
model B
5%
10%
20%
3% melting
model A
field of peridotites
500
200
100
50
20
10
5
Sample / Chondrites
La Ce Nd Sm Eu Gd Dy Er Yb Lu
Rare Earth Atomic Number

REE (Figure 5). If the REE composition of the source peridotite is assumed to be lower the theoretical REE composition of the magma still does not agree well with lamprophyre REE distributions.

The theoretical REE composition of the melt compares much more closely to the actual concentrations in the lamprophyres if a small amount of garnet is included in the residual peridotite mineralogy (Model B). If garnet is added to the mineralogy then hornblende must be removed because these phases are incompatible at pressures in the upper mantle (Kushiro, 1970). With increasing pressure and temperature amphibole breaks down and garnet becomes stable. The H_2O from the hornblende becomes an interstitial vapor phase (Wyllie, 1971). On a temperature versus pressure diagram for peridotite containing 0.1 percent H_2O the phase boundary between hornblende peridotite and garnet peridotite, the solidus, and theoretical geotherm all intersect at roughly 80 kilometers depth and slightly over 1000°C (Wyllie, 1971). If a higher H_2O content and phlogopite are present amphibole would be stable to greater depths (Ringwood, 1975; Wyllie, 1971). As partial melting occured and H_2O was removed from the system amphibole would no longer be stable and the hornblende peridotite could change to a garnet peridotite.

The peridotite mineralogy in the second model for lamprophyre generation (Model B) consists of 0.5 percent phlogopite, 2 percent garnet, 9.5 percent diopside, 23 percent orthopyroxene, and 65 percent olivine. Ito and Kennedy (1967) observed in melting of dry natural peridotite that clinopyroxene is the first phase to melt followed by garnet, orthopyroxene, and olivine. For Model B the author assumed that the phlogopite and diopside preferentially melt followed by constant proportional melting of garnet, orthopyroxene, and olivine. The predicted

compositions of melts generated by 3 percent, 5 percent, 10 percent, and 20 percent partial melting of Model B peridotite are also in Figure 5.

The source peridotite could have been a hornblende peridotite that was being changed to a garnet peridotite at the time of partial melting. Hornblende is required in the model peridotite proposed by Jahn (1973) to explain the K, Rb, Ba, and Sr concentrations in the lamprophyres. Hornblende is not required as a residual phase to explain the K, Rb, Ba, and Sr data, so Model B peridotite is still consistent with these data.

The actual REE compositions of the lamprophyres are very similar to the compositions predicted by 3 to 10 percent partial melting of Model B peridotite. The theoretical REE distributions are generally higher for the intermediate REE than the lamprophyres. The range of REE compositions observed for the lamprophyres could be due to heterogeneity within the peridotite source or different degrees of partial melting. If more olivine is included in the model peridotite, higher REE distributions are produced in the melt. If more garnet is included in the model a steeper curve for the theoretical melt results. The percentage of garnet in the model source must be 1 to 3 percent if the theoretical melt compositions are to match lamprophyric REE compositions for the heavy REE. It is theoretically possible to produce the REE distributions and K, Rb, Ba, and Sr concentrations in the lamprophyres by 3 to 10 percent partial melting of phlogopite-bearing garnet peridotite.

One gabbro sample (44.0 percent SiO_2) was analyzed and has a REE composition similar to the lamprophyres, but slightly lower light REE concentrations (Figure 4b). This rock could have resulted from a higher degree of partial melting (about 20 percent) of the garnet peridotite source which produced the lamprophyric magmas (Figure 5). Partial

melting of peridotite can give rise to basaltic composition melts (Ito and Kennedy, 1967; Kushiro, et al, 1968; Wyllie, 1971; Green, 1973).

Formation of Granitic Rocks of the Main Intrusive Sequence

Granitic melts can be produced by partial melting of a compositionally wide range of materials (Winkler, 1974). Partial melting of high-grade metamorphic rocks can result in water-undersaturated granitic melts (Brown and Fyfe, 1970). Jahn (1973) stated that the granites of the Spanish Peaks complex were derived from partial melting of material in the lower crust. Due to the low Sr^{87}/Sr^{86} initial ratios of these granites, their source could not be the highly radiogenic average Precambrian upper crustal material, but rather the mafic rocks of the amphibolite or granulite facies of the lower crust (Jahn, 1973). Doe (1968) found this to be true for Sr and Pb isotopic data. This model can also be tested with REE data.

The lower continental crust is assumed to be composed of metamorphosed Precambrian continental tholeiites and gabros which after metamorphism to the amphibolite facies could have: 55 percent plagioclase, 30 percent hypersthene, 10 percent hornblende, and 5 percent clinopyroxene.

The REE composition of an average ortho-amphibolite formed from continental tholeiites and gabbros is in Figure 6 (Balashov, et al, 1972). Using the distribution coefficients for silicic rocks of Nagasawa and Schnetzler (1971), Philpotts and Schnetzler (1970), and Schnetzler and Philpotts (1970) as compiled by Arth and Hanson (1975) and the partial melting relationships of Haskin, et al, (1970), assuming modal fractional melting, the theoretical REE compositions of magmas generated by 10 percent, 20 percent, and 30 percent partial melting of this amphibolite were cal-

culated and are in Figure 6 along with the range of values for the three granite samples with higher REE content.

These distributions are similar to those obtained for East Spanish peak, Dike #78, and Dike #87. The variations from the theoretical distributions, such as the size of the negative Eu anomaly or the higher heavy REE concentrations in East Spanish Peak may be reasonably explained by variations in the mineralogy, percent melting, or REE concentrations of the source amphibolite. For example, if the amount of hornblende is increased relative to the other minerals in the model amphibolite the REE concentrations in the hypothetical melt are reduced, especially for the intermediate to heavy REE, and the negative Eu anomaly is reduced.

Formation of Silicic Rocks of Satellite Intrusions

The REE distributions of South White Peak, Mount Mestas, Stock #5, and Plug #16 do not have the same pattern as the other granites. These satellite granites plot at the extreme alkali-rich end of the trend on the AFM diagram except for South White Peak which has lower alkalis and a higher REE distribution. These granites also have fewer mafic minerals than other granites of the complex.

The anomalously low REE contents of these granites are consistent with formation of these magmas by partial melting of peridotite which is depleted in REE in the mantle, because granitic melts are usually enriched in the REE relative to the source. However, there is dispute about the possibility of producing a silicic melt from the partial melting of peridotite. Experimental studies of Kushiro (1970) and Kushiro, et al (1972) indicate that a quartz-normative liquid can be produced by partial melting of a hydrous peridotite. Green (1973) stated that silicic magmas cannot be derived from partial melting of

Figure 6

Theoretical REE compositions of melts formed by 10 percent (upper line), 20 percent, and 30 percent (lower line) partial melting of medel amphibolite (open circles). The range of REE compositions from this study for the main sequence granitic rocks is shaded.

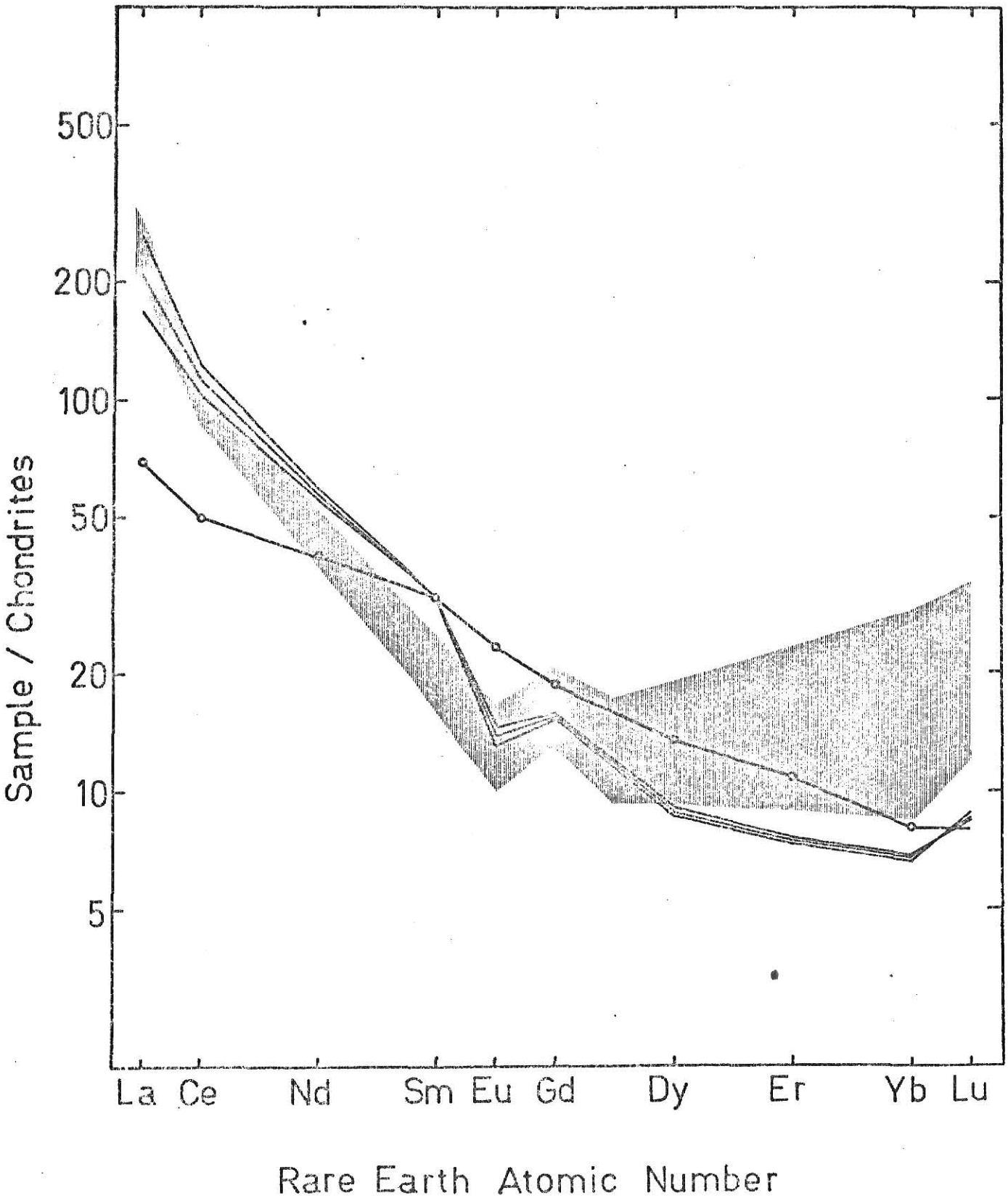
500
200
100
50
20
10
5
Sample / Chondrites
La
Ce
Nd
Sm
Eu
Gd
Dy
Er
Yb
Lu
Rare Earth Atomic Number

peridotite and that experimental silicic liquids are due to the disequilibrium crystallization of olivine on quenching. The Sr^{87}/Sr^{86} initial ratios obtained for the Mount Mestas, South White Peak, and Plug #16 samples (0.7070-0.7079) are within the range of reported values for peridotites, but Sr^{87}/Sr^{86} initial ratios for most pristine peridotites are believed to be lower than these values (Faure and Powell, 1972). The Sr^{87}/Sr^{86} initial ratios for these samples are the same as those determined by Jahn (1973) for other granites in the complex within the error limits, suggesting a similar origin for all the granites. These ratios are too low to have formed from average Precambrian upper crust.

Another possiblity considered is that the REE, especially the light REE, were removed from the magma at the time of emplacement by metasomatic solutions from the intrusion. This might be possible because the granites with anomalously low REE contents are fine-grained and could have formed by the rapid removal of water from the magma at the time of crystallization. This possibility, however, tends to be refuted by the work of Kovalenko, et al (1966) who found that the heavy REE seem to be more mobile than light REE in metasomatic solutions.

A third possiblity is that these anomalous granites, like the other silicic rocks, were also derived from the partial melting of amphibolite, but their low REE contents were controlled by mineral phases such as amphibole, apatite, monazite, or allanite that would reduce the amount of REE in the melt relative to the residual solid. Thus, if the source had a variable residual mineralogy, large variations in REE content of the silicic melts could result. Examples of variations of REE content produced in silicic melts by variation of some of the above minerals will be given in the rest of this section.

Lyakhovich (1967) showed that in monazite-bearing granites monazite contains 40 percent to 90 percent of the total REE content. The same may be true for monazite in some mafic metamorphic rocks, because monazite is abundant in some metamorphic rocks (Vlasov, 1966). Monazite is a REE phosphate which incorporates the lighter REE and rejects Eu and the heavier REE (Vlasov, 1966). Allanite is another REE mineral with chemical affinities similar to monazite.

If a melt formed from the partial melting of an amphibolite and was in equilibrium with a fraction of a percent monazite the melt would be highly depleted in the light REE. If a few percent apatite were included in the mineralogy of the amphibolite this would result in a melt depleted in REE, especially the intermediate REE. The rejection of Eu by the monazite and apatite could be counteracted by the plagioclase concentrating the Eu thus, no net Eu anomaly would result. For example, if we assume an initial mineralogy of 1 percent allanite, 5 percent clinopyroxene, 30 percent hornblende, 30 percent hypersthene, and 34 percent plagioclase for the amphibolite, 3 percent modal partial melting would result in a magma with REE composition A (Figure 7). This REE distribution is similar to those for samples #5 and #16. If we assume a mineralogy of 6 percent apatite, 5 percent clinopyroxene, 10 percent hornblende, 30 percent hypersthene, and 49 percent plagioclase for the amphibolite, the magma formed by 3 percent modal partial melting would have the REE composition B (Figure 7). The REE composition of South White Peak is similar to composition B. This, different amounts of allanite, apatite, and amphibole in the amphibolite source and small degrees of partial melting could result in production of the entire range of REE contents of the granites.

Figure 7

Theoretical REE compositions of melts formed by 3 percent partial melting of model amphibolite (open circles) of compositions A and B. The range of REE compositions from this study for the anomalous satellite granites is shaded.

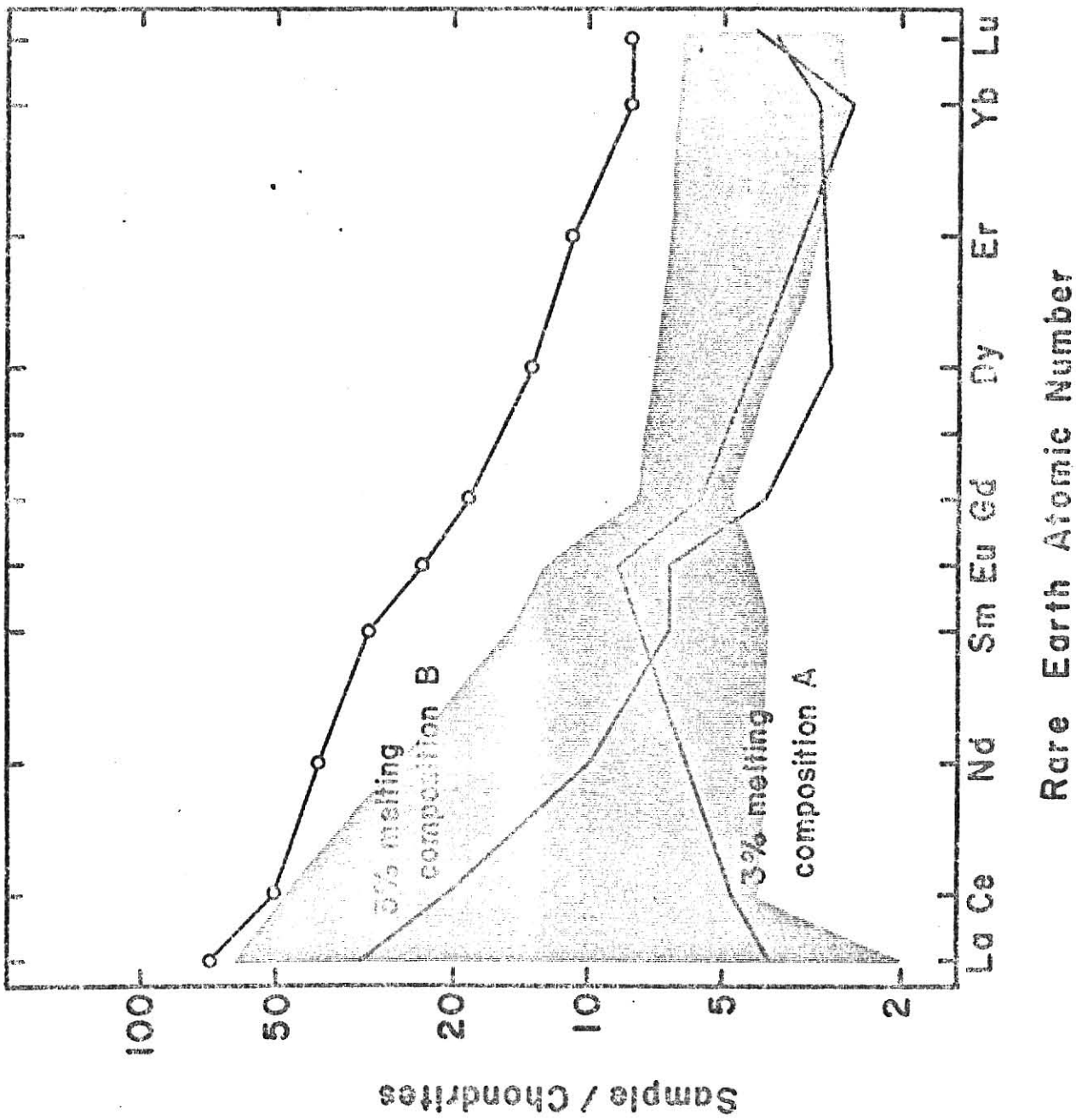
Sample / Chondrites
100
50
20
10
5
2
La Ce Nd Sm Eu Gd Dy Er Yb Lu
Rare Earth Atomic Number
5% melting
composition B
3% melting
composition A

Partial melting of peridotite might explain the low REE contents in the granites, yet tends to be refuted by experimental petrology. Partial melting of amphibolite containing minor phases such as allanite, apatite, and hornblende seems to be the most reasonable model for the production of the granites with anomalously low REE contents. Other minor mineral phases may also cause the fractionation of the REE into the residual phase. Distribution coefficients for the REE are not available for many minor phases which might occur in mafic amphibolites.

Formation of the Intermediate Rocks

The igneous rocks of the Spanish Peaks complex form a complete chemical gradation from the silicic granites to the ultramafic lamprophyres. Jahn (1973) suggested that the intermediate rocks were formed by the mixing of two independent magmas, granitic and lamprophyric which would explain the Sr isotopic data, the K, Rb, Ba, and Sr concentrations and the alkali-rich rocks of intermediate composition. The total REE contents (Table 7) for the different rock types are consistent with this mixing model and the REE distributions for the intermediate rocks are generally between the lamprophyric and granitic REE distributions on the chondrite normalized graphs. On the AFM diagram most intermediate samples fall on a general trend between granites and lamprophyres, but several intermediate and mafic samples lie outside this trend. Samples #86, #108, and #113 are between the granitic field and the lamprophyric field of the AFM diagram and sample #137 is not. Sample #137 has the least SiO_2 of the intermediate rocks and may have a different origin than the other intermediate rock samples. The samples that fall outside the trend on the AFM diagram could not have formed by direct mixing of granitic and lamprophyric magmas.

Perhaps some or all intermediate rocks formed by higher degrees of partial melting of the same amphibolite which produced the granitic magmas. The distribution coefficients for the REE for hornblende are a function of the melt composition and range widely from granitic melts to basaltic melts (Appendix III). In Figure 6 the REE distribution coefficients used for hornblende are for hornblende that is in equilibrium with a silicic melt. In Figure 8, the REE compositions of theoretical melts produced by 10 percent, 20 percent, 30 percent, and 40 percent partial melting of amphibolite with a mineralogy of 55 percent, plagioclase, 30 percent hypersthene, 10 percent hornblende, and 5 percent clinopyroxene are plotted along with the range of REE distributions for the intermediate rocks. For this model the REE distribution coefficients for hornblende were assumed to be an average of distribution coefficients for silicic melts and mafic melts. The REE compositions in the intermediate samples could be produced by 20 percent to 40 percent partial melting of the amphibolite. This model seems more appropriate than the mixing model of Jahn (1973) because the intermediate intrusions are quite voluminous compared to the silicic and mafic intrusions.

CONCLUSIONS

Jahn (1973) stated that the lamprophyres at Spanish Peaks formed from the partial melting of phlogopite-bearing hornblende peridotite in the upper mantle, that the granites formed by partial melting of amphibolite or granulite in the lower crust, and that the intermediate compositions formed by mixing of these two independant magmas. This study supports Jahn's model with certain modifications.

Figure 8

Theoretical REE compositions formed by 10 percent, 20 percent, 30 percent, and 40 percent partial melting of model amphibolite using intermediate distribution coefficients for hornblende. The amphibolite source REE distribution is plotted as open circles. The range of REE compositions for the intermediate rock types from this study is shaded.

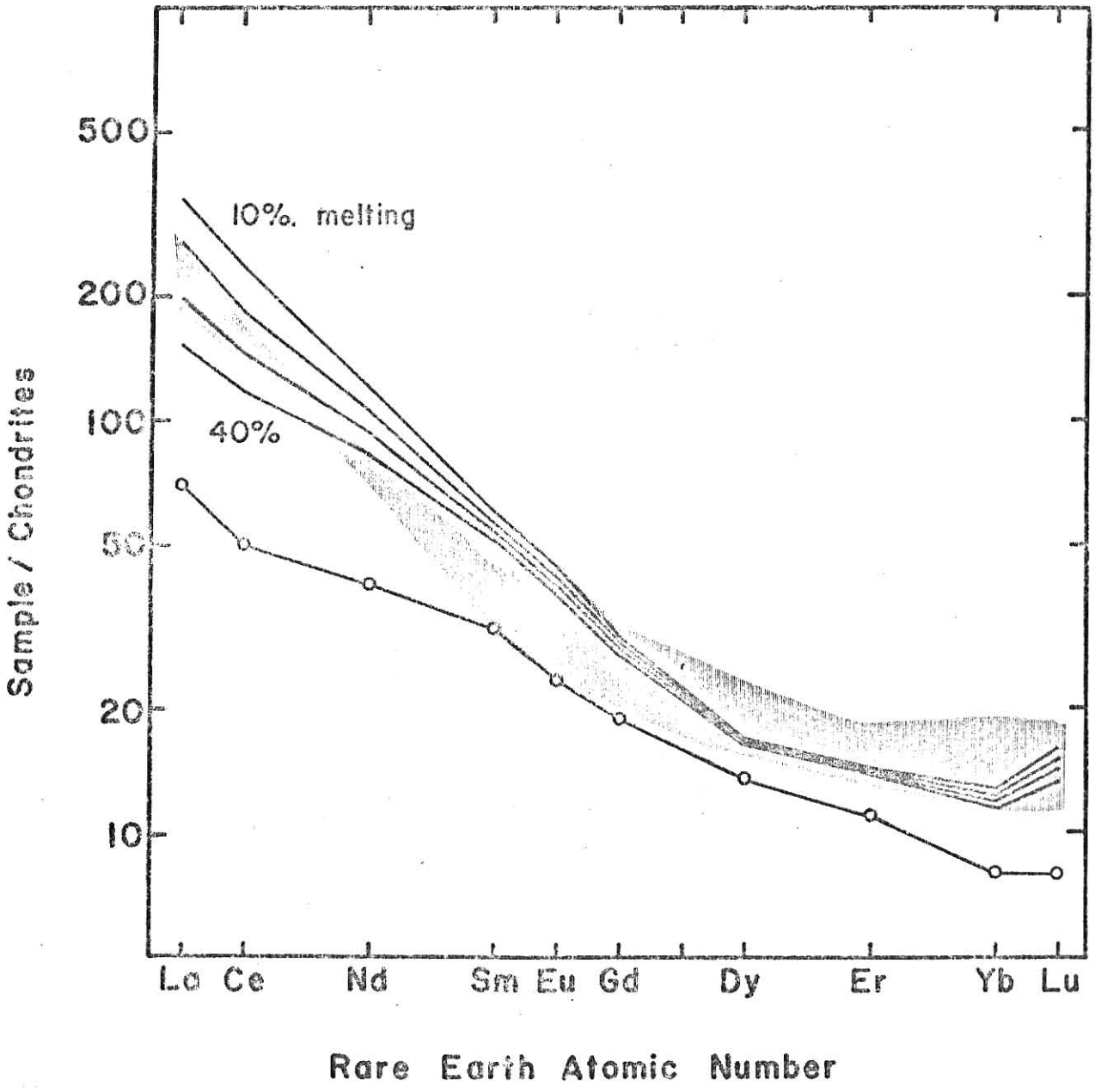
500
200
100
50
20
10
10%. melting
40%
Sample / Chondrites
La Ce Nd Sm Eu Gd Dy Er Yb Lu
Rare Earth Atomic Number

The lamprophyres formed by 3 to 10 percent partial melting of phlogopite-bearing garnet peridotite in the upper mantle. REE data indicate that garnet is a necessary mineral in the residual phase after partial melting of the peridotite. The mafic rocks originated by higher degrees of partial melting of the same peridotite source as the lamprophyres. The granitic rocks formed from the partial melting of amphibolite in the lower crust. The silicic rocks with anomalously low REE contents could have come from the partial melting of amphibolite with different amounts of minor phases such as allanite, monazite, apatite, and hornblende. The intermediate rocks formed in some cases by the mixing of granitic and lamprophyric magmas or, alternately, by higher percentages of partial melting of the amphibolite than that necessary for the generation of the silicic melts.

APPENDIX I

Petrographic Descriptions

Thin sections of the author's samples are described below. Mineral percentages were obtained by visual estimates.

South White Peak:

A light gray, holocrystalline granite composed of 15 percent anhedral quartz (.1-1.0 mm.), 45 percent subhedral orthoclase (0.04-1.0 mm.), 30 percent subhedral zoned oligoclase (An_{28}; 0.05-0.6 mm.), 5 percent subhedral brown biotite (0.1-0.6 mm.), 2 percent subhedral hornblende (0.2-1.0 mm.), and 1 percent subhedral magnetite (0.05-0.2 mm.).

Stock #5:

A gray, fine-grained, holocrystalline granite with 20 percent anhedral quartz as phenocrysts and in the groundmass (0.01-0.5 mm.), 60 percent subhedral orthoclase (0.01-0.2 mm.), 10 percent anhedral plagioclase (0.01-0.1 mm.), 8 percent alteration minerals, and 2 percent subhedral magnetite (0.02-0.1 mm.).

Plug #16:

A very fine-grained, off-white, holocrystalline microgranite with 10 percent anhedral quartz (0.05-0.1 mm.), 50 percent subhedral and euhedral orthoclase as phenocrysts and in the groundmass (0.05-0.7 mm.), 35 percent anhedral antiperthite (0.01-0.02 mm.), 1 percent secondary calcite (0.05-0.1 mm.), and 1 percent subhedral biotite (0.01-0.2 mm.).

Dike #97:

A light brown, holocrystalline minette composed of 30 percent altered subhedral orthoclase (0.02-0.1 mm.), 20 percent subhedral oligoclase

(0.02-0.08 mm.), 35 percent subhedral red biotite phenocrysts (0.1-2.0 mm.), 3 percent subhedral green augite (0.05-0.3 mm.), 1 percent anhedral olivine (0.02-0.1 mm.), 6 subhedral altered magnetite (0.05-0.6 mm.), and 1 percent calcite (0.05-0.3 mm.).

Dike #168:

A dark gray, holocrystalline odinite with 10 percent anhedral orthoclase (0.05-0.1 mm.), 20 percent subhedral labradorite (0.02-0.4 mm.), 15 percent clays, 4 percent subhedral biotite (0.01-0.05 mm.), 5 percent euhedral magnetite (0.01-0.07 mm.), 10 percent subhedral apatite (0.02-0.3 mm.), 8 percent anhedral calcite (0.02-0.1 mm.).

Dike #173:

A dark gray, holocrystalline monchiquite containing 40 percent euhedral titanaugite (0.05-1.0 mm), 25 percent subhedral labradorite (An_{52}) (0.02-0.5 mm.), 20 percent anhedral orthoclase (0.01-0.05 mm.), 5 percent subhedral biotite (0.01-0.1 mm.), 3 percent subhedral magnetite (0.01-0.05 mm.). 5 percent chlorite (0.01-0.1 mm.).

The following samples were analyzed for the REE and were obtained from Ross Johnson, U.S.G.S., Denver, Colorado. These petrographic descriptions are summarized from Johnson (1968).

East Spanish Peak:

A very light gray granite porphyry with 40 percent anorthoclase with phenocrysts up to 10 mm., 31 percent oligaclase (An_{25}) with phenocrysts as much as 3.5 mm. across, 17 percent anhedral to subhedral quartz, 2-5 percent biotite and hornblende, 19-31 percent groundmass, and 9 percent microperthite.

Mount Mestas:

A very light gray holocrystalline microgranite with 20 percent quartz, 60 percent anorthoclase, 17 percent oligoclase (An_{15}), 2 percent magnetite, and traces of biotite, limonite, chlorite, and clay.

Dike #78:

A granite porphyry with the following ranges in composition: 5-15 percent quartz, 30-50 percent orthoclase, 30-38 percent oligoclase (An_{20}), 2-6 percent biotite, 0-3 percent hornblende, 1-5 percent magnetite, and traces of corundum.

Dike #87:

A granodiorite porphyry with phenocrysts of oligoclase, microcline, biotite, and hornblende. Modal composition is 8 percent quartz, 28 percent orthoclase, 1 percent microcline, 45 percent oligoclase, 4 percent biotite, 1 percent hornblende, 3 percent magnetite and ilmenite, <1 percent apatite and corundum, and 10 percent secondary minerals.

Dike #86:

A light gray syenite porphyry with phenocrysts of oligoclase, augite, and red biotite. Modal analysis is 1 percent quartz, 45 percent orthoclase, 36 percent oligoclase (An_{30}), trace of biotite, 4 percent augite, 3 percent amphibole, traces of corundum and apatite, 3 percent magnetite, trace of limonite, 3 percent calcite, 3 percent clay, and trace of zeolite.

Dike #108:

A light gray syenodiorite porphyry containing phenocrysts of oligoclase, hornblende, and augite. The composition is 15 percent orthoclase,

45 percent oligoclase (An_{25}), 3 percent red biotite, 2 percent green hornblende, 4 percent green augite, 1 percent apatite, 5 percent magnetite and ilmenite, 3 percent limonite, 4 percent chlorite, and 17 percent zeolite.

Dike #113:

A light, medium gray syenodiorite prophyry with pehnocrysts of hornblende and oligoclase. Modal composition is 2 percent quartz, 12 percent orthoclase, 41 percent oligoclase (An_{25}), 9 percent hornblende, 6 percent augite, 1 percent biotite, traces of apatite and sphene, 11 percent magnetite, 6 percent chlorite, trace of epidote, 5 percent zeolite, and 4 percent clay.

Dike #137:

A medium, dark gray microsyenodiorite composed of 6 percent orthoclase, 31 percent andesine (An_{40}), 2 percent biotite, 8 percent augite, 6 percent acmite(?), 3 percent magnetite and ilmenite, 3 percent apatite, 5 percent calcite, 4 percent clay, 25 percent chlorite, and 7 percent limonite.

Dike #178:

A medium olive-brown gabbro porphyry with phenocrysts of labradorite (24 percent) (An_{60}), 4 percent red biotite, 5 percent red hornblende, 20 percent green augite, 1 percent apatite, 12 percent magnetite and ilmenite, 12 percent chlorite, 2 percent calcite, and 4 percent zeolite.

APPENDIX II

Experimental Methods

Major Element Analysis by Atomic Absorption Spectrophotometry

Samples were dissolved in HF acid and aqua regia in a teflon-lined bomb and diluted for analysis. Exactly 0.1000±0.0002 gram of powdered sample was weighed into the teflon cup of the bomb. Using a small graduated cylinder, 6 ml. of concentrated HF acid and 1 ml. aqua regia were added to each sample. The bomb was then sealed and placed in a drying oven at 110°C for approximately 45 minutes or until all the material was dissolved to visible inspection. After being allowed to cool to room temperature, the bomb was opened and the sample was checked for complete dissolution. The sample was quantitatively transferred to a teflon beaker containing 4.00 grams of boric acid, about 75 ml. of distilled-deionized water were added, and the solution was stirred with a teflon stirring rod until the boric acid was dissolved. The solution was transferred to a 200 ml. volumetric flask and 1 ml.± 0.01 ml. of La Stock solution was pipetted into the flask. After dilution to 200 ml. the solution was stored in a polyethylene bottle.

The La Stock solution was prepared by dissolving $LaCl_3 \cdot 6H_2O$ in distilled-deionized water to obtain the concentration of 4986 ugm./ml.

A blank solution, used as a zero reference for the analyses, was prepared by combining 6 ml. HF acid, 1 ml. aqua regia, 4.00 grams of boric acid, and 1 ml. of La stock solution and diluting to 200 ml.

Two combined standard solutions were prepared to approximate the composition of a granite and a lamprophyre (Table 8). Commercially

Table 8

Standards for Atomic Absorption Spectrophotometry

element	Granite Standard concentration (ppm)	Lamprophyre Standard concentration (ppm)
Al	50	50
Fe	10	60
Mg	4	40
Ca	10	70
Na	20	20
K	20	20
Sr	1	6
Ba	2	5
Rb	1	1

obtained standard solutions of 1000 mg./l. concentration of different elements were pipetted together and diluted with blank solution to prepare these standards. Another standard was prepared for both the granite and the lamprophyre standards by diluting these 1:2 with blank.

A perkin-Elmer Model 305B atomic absorption spectrophotometer was used for the analyses. Analyses for Si, Al, Fe, Na, K, and Ca were performed with stock sample solutions. Some sample solutions were diluted 1:5 for analyses of Mg. For the analysis of Na, K, Sr, and Ba a solution of RbCl was added to all samples, standards, and blank. The resulting concentration of about 1000 mg./l. Rb helped to eliminate ionization interferences of these elements in the flame. Table 9 gives the instrument settings for the analyses of the different elements.

The following changes in AA techniques are noted to improve results. The analyses for Al were done on the stock sample solutions and analyses for Ca, Fe, Mg, and Na were performed with a solution diluted 1:10 from the stock sample solution and containing 1000 mg./l. K and 1000 mg./l. Sr. The La solution was omitted from the procedure. The analyses for K were done with a solution diluted 1:10 from the stock solution and containing 1000 mg./l. Na. The Sr was added to eliminate ionization interferences for Ca and Mg, while the K did the same for Na analyses and Na for the K analyses. Stock solutions of 10,000 mg./l. Sr, K, and Na were prepared using $SrCO_3$, KCl, and NaCl.

The samples were diluted to a concentration of 40-60 ppm Sr for the analyses of Si. Each sample solution was run at least five times and alternated with a standard solution between each sample solution run. The flame was adjusted to be only slightly reducing with no carbon

TABLE 9

Instrument Settings for Atomic Absorption Spectrophotometer

Element	Wavelength (Å)	Slit	Burner orientation	Burner position height	Gas flow rate C_2H_2	air	N_2O	Wavelength range	Function
Si	252.8	3	perpendicular	6.0	5.5		5.0	UV	absorption
Al	309.2	4	perpendicular	7.0	5.0		5.0	UV	absorption
Fe	248.5	3	perpendicular	7.0	5.0	5.0		UV	absorption
Mg	285.3	4	perpendicular	5.3	5.0	5.0		UV	absorption
Ca	211.4	4	perpendicular	7.0	4.5	5.0		Vis	absorption
Na	294.5	4	perpendicular	3.0	5.0	5.0		Vis	emission
K*	382.9	4	perpendicular	4.5	5.1	5.9		Vis	emission
Ti	399.6	3	parallel	7.1	5.2		5.0	UV	emission

* red filter used.

build-up on the burner head. The more oxidizing flame reduces the sensitivity for Si but results in a more stable flame and better results.

Mass Spectrometry

Mass spectrometry techniques were adapted from Methot (1973). Powdered samples were dissolved in hydrofluoric and perchloric acids in a teflon dish. The samples were evaporated on a hot plate to near dryness and the material was redissolved in 1 Normal hydrochloric acid.

The strontium was separated by a cation-exchange technique using columns of resin. The columns were eluted with 2 Normal hydrochloric acid and the strontium collected in teflon beakers. These samples were concentrated, evaporated to dryness, and heated to oxidize organic residue.

A 6-inch radius, 60° sector mass spectrometer was used to obtain Sr^{87}/Sr^{86} ratios for these samples. The samples were dissolved in 3 Normal nitric acid and evaporated on a tantalum filament.

Values for Rb and Sr concentrations of the whole rock samples were obtained by energy dispersive x-ray fluorescence. A radioactive Cd^{109} x-ray source was used and the x-ray fluorescence was detected by a Si(Li) detector coupled with a 256 channel analyzer. The Rb and Sr peak areas of the samples and standards were determined by a computer analysis.

This x-ray fluorescence technique is relatively inaccurate in comparison to the standard practice of determining Rb and Sr concentrations by isotope dilution. However, because these rocks are young in relation to the Rb-Sr isotopic system, errors in the Rb and Sr concentrations will have a small effect on (Sr^{87}/Sr^{86}) initial values.

The values reported for (Sr^{87}/Sr^{86}) initial were calculated from the following equation:

$$(Sr^{87}/Sr^{86})_{Initial} = (Sr^{87}/Sr^{86}) - (Rb^{87}/Sr^{86})(e^{\lambda t}-1)$$

The calculations are made with the assumption that the age of the igneous bodies is 25 million years.

Neutron Activation Analysis

Approximately 0.3 grams of powdered samples and liquid standard were weighed to the nearest 0.0001 g. into clean polyethylene vials and the top was heat sealed with a soldering gun. About 50 mg. of Fe wire were weighed to the nearest 0.0001 g. for each sample and standard, and the wires were wrapped spirally around each vial with tape. The Fe wire served as a neutron flux monitor to correct for differences in neutron flux within the reactor core. Most runs consisted of four samples and two standards.

The samples and standards were irradiated for approximately two hours in the core of the General Atomic TRIGA Mark II reactor at a flux of $\sim 10^{13}$ neutrons/cm^2 sec. Samples were left in the reactor pool for between 4 and 24 hours depending on the activity. The samples were then moved to a laboratory for the chemical separation of the REE from the rock samples.

The chemical separation of the REE from a silicate rock sample is described by Denechaud, et al, (1970). The separation technique basically consists of fusion of the rock samples with Na_2O_2 and subsequent dissolution. The REE, Fe, Al, and Si are precipitated as hydroxides and removed by centrifuging. The Si is removed by precipitation with gelatin. The Fe is removed by an ether extraction and the REE are finally precipitated with oxalic acid as REE oxalates. This precipitate is filtered, dryed, and mounted on cardboard counting cards for radio-

assay. The REE oxalates are precipitated directly from the liquid standard and also mounted on a counting card.

The standards and samples were counted on a Ge(Li) gamma detector coupled with a 4096 channel analyzer. Gamma-ray spectra were taken for each sample at about 1-day, 3-day, 10-day, and 40-day intervals after the irradiation. The early count sets were used for the analysis of short half-life REE isotopes and the later sets for longer half-life isotopes.

The Fe wires were counted on the Ge(Li) detector at least two weeks after irradiation. From these data the relative neutron flux which each sample or standard received could be calculated.

The concentration of any given element was calculated from the ratio of the peak areas of the sample to the standard. Correction factors for sample weights, chemical yield, radioactive decay rate, and flux differences also had to be included in the final calculations.

The peak area for a gamma photopeak was calculated by summing the counts in the central seven channels of the peak and subtracting off an average background value from each channel. The average background count for each peak was obtained from hand plotted graphs of the peak. The peak area was corrected for radioactive decay by a factor of $e^{\lambda t}$ where λ is the decay constant of the isotope and t is the time between the standard count and the sample count.

Because the chemical separation of the REE is not quantitative, the final calculations must include a correction for the chemical yield. A given quantity of Y^{88} tracer was added to the samples and standard before the chemical separation. The Y^{88} acts chemically like Dy. The 1.836 Mev peak of Y^{88} was used to monitor the yield of the REE in the chemical separation.

The different REE have different relative yields. A REE carrier of known composition was added to each sample and standard prior to the chemical separation to correct for this fractionation. After the samples had been counted for the 40-day count, they were cut open and about one-eighth of the oxalate was removed. These samples were sealed in plastic and placed in a polyethylene vial for reirradiation. The vials were placed in the rotary specimen rack of the reactor and irradiated for one hour at a flux of approximately 1.6×10^{12} neutrons/cm^2 sec.

After eight days these samples were counted for about one hour on the Ge(Li) detector. The relative chemical yields for the REE was calculated by comparing the peaks of a given element of the sample to the standard. The standard was assumed to have a 100 percent yield. The absolute chemical yield for each element was then calculated and the final concentration for the REE in the samples could be obtained.

The following equation summarizes the calculations:

$$Cs = (As/Am)\ (Gm/Gs)\ (Fm/Fs)\ (Cm/Y)$$

where; Cs = concentration of the element in the sample in ppm

Cm = concentration of the element in the standard in ppm

As = peak area in counts per unit time for the sample

Am = peak area in counts per unit time for the standard

Gs = weight of the irradiated sample in g

Gm = weight of the irradiated standard in g

Fs = cpm/mg for the Fe wire surrounding the sample

Fm = cpm/mg for the Fe wire surrounding the standard

y = absolute chemical yield for the element

from Yeh (1973)

The precision of this radiochemical NAA technique was ± 2 percent for La, Ce, Sm, Eu, Yb, and Lu; ± 5 percent for Tb and Ho; and ± 15 percent for Gd (Denechaud, et al, 1970).

APPENDIX III

DISTRIBUTION COEFFICIENTS*

Distribution coefficients for basaltic and andesitic rocks

	olivine	diopside	hornblende	garnet	ortho-pyroxene	phlogopite
Ce	0.0069	0.070	0.20	0.028	0.024	0.034
Nd	0.0066	0.12	0.33	0.068	0.033	0.032
Sm	0.0066	0.18	0.52	0.29	0.054	0.031
Eu	0.0068	0.18	0.59	0.49	0.054	0.030
Gd	0.0077	0.19	0.63	0.97	0.091	0.030
Dy	0.0096	0.21	0.64	3.17	0.15	0.030
Er	0.011	0.17	0.55	6.56	0.23	0.034
Yb	0.014	0.16	0.49	11.5	0.34	0.042
Lu	0.016	0.13	0.43	11.9	0.42	0.046

Distribution coefficients for rhyolitic rocks

	hypersthene	clinopyroxene	hornblende	plagioclase
Ce	0.15	0.50	1.52	0.27
Nd	0.22	1.11	4.26	0.21
Sm	0.27	1.67	7.77	0.13
Eu	0.17	1.56	5.14	2.15
Gd	0.34	1.85	10.0	0.097
Dy	0.46	1.93	13.0	0.064
Er	0.65	1.66	12.0	0.055
Yb	0.86	1.58	8.38	0.049
Lu	0.90	1.54	5.5	0.046

* taken from Arth and Hanson (1975)

original references: Nagasawa and Schnetzler (1971), Higuchi and Nagasawa (1969), Philpotts and Schnetzler (1970), Schnetzler and Philpotts (1968), and Schnetzler and Philpotts (1970).

ACKNOWLEDGEMENTS

I would like to thank Dr. Robert Cullers for his guidance and assistance in all phases of this study. I also want to thank Dr. Sambhudas Chaudhuri, Dr. Donald Whittemore, Dr. Page Twiss, and Dr. Dean Eckhoff for serving on my advisory committee. I gratefully appreciate the help of Mike McEwan and the staff of the KSU Department of Nuclear Engineering nuclear reactor in irradiating the samples. I also want to thank Sherri Alderman for typing the final draft of this thesis.

REFERENCES CITED

Arth, J. G., and Hanson, G. N., 1975, Geochemistry and origin of the early Precambrian crust of northeastern Minnesota: Geochim. et Cosmoch. Acta., v. 39, p. 325-362.

Balashov, Y. A., Kremenetskiy, A. A., and Shvets, V. M., 1972, Geochemical criteria of the nature of Precambrian amphibolites: Geochem. Int., v. 9, p. 918-931.

Brown, G. C. and Fyfe, W. S., 1970, The production of granitic melts during ultrametamorphism: Contr. Miner. Petr., v. 28, p. 310-318.

Buckley, E. B., and Cranston, R. E., 1971, Atomic absorption analyses of 18 elements from a single decomposition of aluminosilicate: Chem. Geol., v. 7, p. 273-284.

Dawson, J. B., 1971, Advances in kimberlite geology: Earth Sci. Rev., v. 7, p. 187-214.

Denechaud, E. B., Helmke, P. A., Haskin, L. A., 1970, Analysis for the rare-earth elements by neutron activation and Ge(Li) spectrometry: Jour. Radioanalytical Chem., v. 6, p. 97-113.

Doe, Br. R., 1968, Lead and strontium isotopic studies of Cenozoic volcanic rocks in the Rocky Mountain region--a summary: Colorado School of Mines Quarterly, v. 68, p. 149-174.

Epis, R. C. and Chapin, C. E., 1968, Geological history of the thirtynine mile volcanic field, central Colorado: Colorado School of Mines Quarterly, v. 68, p. 51-85.

Faure, G., and Powell, J. L., 1972, Strontium Isotope Geochemistry: New York, Springer-Verlag, 188 pp.

Flanagan, F. J., 1969, U. S. Geological Survey standatds - II. First compilation of data for the new U. S. G. S. rocks: Geochim. et Cosmoch. Acta., v. 33, p. 81-120.

Frey, F. A., Haskin, M. A., Poetz, J., and Haskin, L. A., 1968, Rare earth abundances in some basic rocks: Jour. Geophys. Res., v. 71, p. 6091-6105.

Gordon, G. E., 1968, Instrumental activation analysis of standard rocks with high resolution -ray detectors: Geochim. et Cosmoch. Acta., v. 32, p. 369-396.

Green, D. H., 1973, Experimental melting studies on a model upper mantle composition at high pressure under water-saturated and water-undersaturated conditions: Earth Planet. Sci. Lett., v. 19, p. 37-53.

Green, D. H., and Ringwood, 1967. The genesis of basaltic magmas: Contr. Mineral. and Petrol., v. 15, p. 103-190.

Green, D. H., and Ringwood, A. E., 1968, Genesis of the calc-alkaline igneous rock suite: Contr. Mineral. and Petrol., v. 18, p. 105-162.

Haskin, L. A., Haskin, M. A., Frey, F. A., and Wildeman, T. R., 1968, Relative and absolute terrestrial abundances of the rare earths: Origin and Distribution of the Elements (editor L. H. Ahrens), p. 889-912, Pergamon Press.

Haskin, L. A., Allen, R. O., Helmke, P. A., Paster, T. P., Anderson, M. R., Korotev, R. L., and Zweifel, K. A., 1970, Rare earths and other trace elements in Apollo 11 lunar samples: Proceedings of the Appollo 11 Lunar Science Conference, v. 2, p. 1213-1231.

Hertogen, J., and Gijbels, R., 1976, Calculation of trace element fractionation during partial melting: Geochim. et Cosmoch. Acta., v. 40, p. 313-322.

Higuchi, H. and Nagasawa, H., 1969, Partition of trace elements between rock-forming minerals and the host volcanic rocks: Earth Planet. Sci. Lett., v. 7, p. 281-287.

Ito, K., and Kennedy, G. C., 1967, Melting and phase relations in a natural peridotite at 40 kilobars: Am. Jour. Sci., v. 265, p. 519-538.

Jahn, B., 1973, A petrogenetic model for the igneous complex in the Spanish Peaks region, Colorado: Contr. Miner, Petr., v. 27, p. 1-16.

Johnson, R. B., 1961, Patterns and origin of radial dike swarms associated with West Spanish Peak and Dike Mountain, south-central Colorado: Geol. Soc. Am. Bull., v. 72, p. 579-590.

Knopf, A., 1936, Igneous geology of the Spanish Peaks region, Colorado: Geol. Soc. Am. Bull., v. 47, p. 1727-1784.

Kovalenko, V. I., Znamenskaya, A. S., Afonin, V. P., Pavlinskiy, G. V., and Makov, V. M., 1966, Behavior of rare earth elements and yttrium in metasomatically altered alkalic granites of the Ognitsk complex (East Sayan): Geochem, It., v. 3, p. 406-418.

Kushiro, I., 1970, Systems bearing on melting of the upper mantle under hygrous conditions: Carnegie Inst. Wash. Yr. Book, v. 68, p. 240.

Kushiro, I., Syono, Y., and Akimoto, S., 1968, Melting of a peridotite nodule at high pressures and high water pressures: Jour. Geophys. Res., v. 73, p. 6023-6029.

Loubet, M., Shimizu, N., and Allegre, C. J., 1975, Rare earth elements in alpine peridotites: Contr. Miner. Petr., v. 53, p. 1-12.

Lyakhovich, V. V., 1967, Distribution of rare earths among the accessory minerals of granites: Geokhimiya, no. 7, p. 828-933.

Methot, R. L., 1973, Internal geochronologic study of two large permatites, Connecticut: Kansas State University, Ph. D. dissertation, 123p.

Miyashiro, Al, 1973, Metamorphism and metamorphic belts: New York, John Wiley and Sons, 492 p.

Nagasawa, H., and Schnetzler, C. C., 1971, Partitioning of rare earth, alkali, and alkali earth elements between phenocrysts and acidic igneous magma: Geochim. et Cosmoch. Acta., v. 35, p. 953-968.

Nagasawa, H., Wakita, H., Higuchi, H., and Onuma, N., 1969, Rare earths in peridotite nodules: an explanation of the genetic relationship between basalt and peridotite nodules: Earth Planet. Sci. Lett., v. 5, p. 377-381.

Ode, H., 1957, Mechanical analysis of the dike pattern of the Spanish Peaks area, Colorado: Geol. Soc. Am. Bull., v. 68, p. 567-576.

O'Hara, M. J. and Yoder, H. S., 1967. Formation and fractionation of basic magmas at high pressures: Scot. Jour. Geol., v. 3, p. 67-117.

Philpotts, J. A. and Schnetzler, C. C., 1970, Phenocryst-matrix partition coefficients for K, Rb, Sr, and Ba with applications to anorthosite and basalt genesis: Geochim. et Cosmoch. Acta, v. 34, p. 307-322.

Philpotts, J. A., Schnetzler, C. C., and Thomas, H. H., 1972, Petrogenetic implications of some new geochemical data on eclogitic and ultrabasic inclusions: Geochim. et Cosmoch. Acta, v. 36, p. 1131-1166.

Philpotts, J. A., Schnetzler, C. C., and Hart, Sr. R., 1970, Submarine basalts: some K, Rb, Sr, Ba and rare-earth data bearing on their alteration, modification by plagioclase, and possible source materials: Earth Planet, Sci. Lett., v. 7, p. 293-299.

Ramlala, R. T., and Loring, D. H., 1975, Multi-element analysis of silicate rocks and marine sediments by atomic absorption spectrophotometry: Atomic Absorption Newsletter, v. 14, p. 117-120.

Reid, J. B. and Frey, F. A., 1971, Rare earth distributions in lherzolite and garnet pyroxenite xenoliths and the constitution of the upper mantle: Jour. Geophys. Res., v. 76, p. 1184-1196.

Ringwood, A. E., 1975, Composition and petrology of the earth's mantle: New York, McGraw-Hill, 618p.

Ronov, A. B., Balashov, Y. A., and Migdisov, A. A., 1967, Geochemistry of rare earths in the sedimentary cycle: Geochem. Int., v. 4, p. 1-17.

Schnetzler, C. C. and Philpotts, J. A., 1968, Partition coefficients of rare-earth elements and barium between igneous matrix material and rock-forming-mineral phenocrysts-I: Pergamon Press, Origin and Distribution of the Elements, (editor L. H. Ahrens), p. 929-938.

Schnetzler, C. C., and Philpotts, J. A., 1970, Partition coefficients of rare-earth elements between igneous matrix material and rock forming mineral phenocrysts-II: Geochem. et Cosmoch. Acta, v. 34, p. 331-340.

Siems, P. L., 1968, Volcanic geology of the Rosita Hills and Silver Cliff district, Custer County, Colorado: Colorado School of Mines Quarterly, v. 63, p. 89-124.

Stormer, J. C., 1972, Ages and nature of volcanic activity on the southern High Plains, New Mexico and Colorado: Geol. Soc. Am. Bull., v. 83, p. 2443-2448.

Van de Kamp, P. C., 1970, The green beds of the Scottish dalradian series: geochemistry, origin, and metamorphism of mafic sediments: Jour. Geol., v. 78, p. 281-303.

Vlasov, K. A., 1966, Geochemistry and mineralogy of rare elements and genetic types of their deposits: v. II, Jerusalem, Isreal Program for Scientific Translations, 945 p.

Winkler, H. G., 1974, Petrogenesis of metamorphic rocks: New York, Springer-Verlag, 237 p.

Wyllie, P. J., 1971, Role of water in magma generation and initiation of diapiric uprise in the mantle: Jour. Geophys. Res., v. 76, p. 1328-1338.

Wyllie, P. J., 1971, The Dynamic Earth: Textbook in Geosciences: New York, John Wiley and Sons, Inc., 416 p.

Yeh, L., 1973, The distribution of the rare earth elements in Silurian pelitic schists from northwestern Maine: Kansas State University, M. S. Thesis, 48 p.

PETROGENESIS OF THE SPANISH PEAKS IGNEOUS COMPLEX, COLORADO: MAJOR ELEMENT, RARE EARTH ELEMENT, AND STRONTIUM ISOTOPIC DATA

by

Bill W. Arnold

B. S., Kansas State University, 1973

AN ABSTRACT OF A MASTER'S THESIS

submitted in partial fulfillment of the

requirements for the degree

MASTER OF SCIENCE

Department of Geology

KANSAS STATE UNIVERSITY
Manhattan, Kansas

1977

ABSTRACT

The Spanish Peaks igneous complex, south-central Colorado, consists of Tertiary intrusive rocks which range from lamprophyric to granitic in composition and form two main stocks surrounded by a radial dike swarm and other smaller stocks and plugs. Partial melting of phlogopite-bearing hornblende peridotite to form the lamprophyres and partial melting of amphibolite or granulite as the origin of the granites has been proposed by Jahn (1973) for the Spanish Peaks complex. Jahn (1973) stated that the intermediate rocks formed from the mixing of the independent lamprophyric and granitic magmas. To test Jahn's model representative samples were analyzed for major element composition and Sr^{87}/Sr^{86} initial ratios. REE concentrations for the lamprophyres are generally high for the light REE and low for the heavy REE with high La/Lu ratios (84.3-200 ppm La; .31-.38 ppm Lu; average La/Lu=353). For intermediate rocks the REE concentrations are lower than the lamprophyres for the light REE (55.7-80.3 ppm La; .36-.58 ppm Lu; average La/Lu=149). Concentrations in the main sequence granites are somewhat lower still (58.0-83.6 ppm La; .35-1.02 ppm Lu; average La/Lu=156). Several silicic rocks having anomalously low REE contents were analyzed (.59-18.8 ppm La; .08-.21 ppm Lu; average La/Lu=13.3). The range of Sr^{87}/Sr^{86} initial ratios for three of the anomalous granites is 0.7070-0.7079.

The data from this study used in conjunction with the results of Jahn (1973) indicate that the lamprophyres of the complex formed by 3 to 10 percent partial melting of phlogopite-bearing garnet peridotite in the upper mantle. The silicic rocks originated from 10 to 30 percent partial melting of amphibolite in the lower crust derived from metamorphosed

continental tholeiites and gabbros. The silicic rocks with anomalously low REE contents could have formed from the partial melting of amphibolite with different amounts of allanite, monazite, apatite, and hornblende. The intermediate rocks formed in some cases by the mixing of granitic and lamprophyric magmas or, alternately, by greater degrees of partial melting of the amphibolite than that necessary for the generation of the silicic melts.